Nonlinear Dyn (2018) 94:1267–1275
https://doi.org/10.1007/s11071-018-4422-8

ORIGINAL PAPER

Phase transition in coupled star networks

Can Xu · Yuting Sun · Jian Gao · Wenjing Jia · Zhigang Zheng

Received: 11 March 2018 / Accepted: 12 June 2018 / Published online: 18 June 2018

Abstract Collective behaviors of coupled oscillators are an important issue in the field of nonlinear dynamics and complex networks, which have attracted much attention in recent years. For some systems satisfying certain symmetries, the dynamics of high-dimensional space can be reduced to that of low-dimensional subspace in terms of the Watanabe–Strogatz theory. In this paper, the dynamics of the transition to synchronization on the coupled star networks are studied, and we identify a two-step phase transition in the system both from the macroscopic and from the microscopic viewpoints. Theoretically, the low-dimensional order-parameter dynamical equation is developed to get analytical insights, and the roles of the coupled hubs in the synchronization process are uncovered. Physically, the two-phase transition steps correspond to different bifurcations in phase space. Theoretical analysis is examined by performing the numerical simulations, and the results and analysis proposed in this paper are helpful to understand the phase transition in general heterogeneous networks.

C. Xu · W. Jia · Z. Zheng (✉)
Institute of Systems Science and College of Information Science and Engineering, Huaqiao University, Xiamen 361021, China
e-mail: zgzheng@hqu.edu.cn

Y. Sun
Department of Physics, Beijing Normal University, Beijing 100875, China

J. Gao
Johann Bernoulli Institute for Mathematics and Computer Science, University of Groningen, P.O. Box 407, Groningen 9700 AK, The Netherlands

Keywords Coupled oscillators · Phase transition · Synchronization · Star network

1 Introduction

Collective behaviors of the coupled rhythmic units have become an important issue in various fields that range from chemistry, physics, ecology, neuron, and even to social system [1–8]. Further studies show that the evolutions and formulations of such cooperative phenomena are closely related to the intrinsic structure of the systems. The relationships between the topological structure and the functions of the system have become a significant topic in the scientific community which attracted much attention along the past decades [9–16].

A typical example in this area is an abrupt phase transition to synchronization in scale-free networks with considering the positive correlation between the natural frequency of node oscillators and the degree of nodes [13]. This explosive synchronization has been found in various networks by setting appropriate conditions and experimentally implemented in electronic circuits [17,18]. A variety of efforts have been made to explore the microscopic mechanisms of such dynamical process, for instance the heterogeneous structures of networks, the coupling functions between oscillators, and even the role of asymmetry in the natural frequency distributions and so on [18–22].

In coupled phase oscillators with various network structures, the size of the system is always very large, and hence, the phase space for description of the nodes' dynamics is high dimensional which leads to the difficulty in mathematical treatment. As a result, the dimensional reduction technique is necessary for depicting the system in a much lower-dimensional subspace, especially when the dynamical equations have some properties of symmetry, such as the significant work of Ott and Antonsen [24]. In [24], the authors pointed out that for the generalized Kuramoto model with an infinite size, the system has an invariant submanifold for the long-time evolution which can be described in terms of several coupled ordinary differential equations (ODEs). However, in the network with a finite size, the Ott–Antonsen ansatz can still be used to grasp the essential dynamical characteristics of the system by the developed Watanabe–Strogatz approach [25,26].

In heterogeneous networks, hubs usually play an important role in the dynamical transition to synchronization. The single star network is very useful to understand the main behaviors of heterogeneous networks [23,27,29–31]. However, many heterogeneous networks have multiple hubs, and these hubs interact with each other. In this paper, to investigate the influence of hubs on synchronization, we consider the simplest case of the heterogeneous networks, i.e., the coupled star networks. Surprisingly, we observe a particular phase transition to synchronization that is much different from the situation in a single star network [23]. In general, the phase transition in the coupled star network can be divided into two steps. At the first step, the transition is from the incoherent state to the in-phase state where all the leaf nodes in each star form a synchronized group with the same phase; at the second step, the system gradually becomes globally synchronized when the coupling strength among hubs is large enough. Further theoretical analysis indicates that the former is closely associated with the coupling between hubs, which accelerates the synchronization process in each single star network.

The paper is organized as follows: The coupled star network is introduced, and a two-step phase transition to synchronization is found in Sect. 2. In Sect. 3, we extend the Watanabe–Strogatz approach and propose the governing equation for networks with a finite size. To get some analytical insights of the transition mechanism, in Sect. 4, we reduce the original dynamical equations into a simple model. It is revealed that the first step of phase transition is the bifurcation from the chaotic or quasiperiodic torus to a limit cycle in the phase space. This conclusion can be further verified by the linear relation between the critical point and the initial order parameter. Finally, the last section is devoted to a summary and discussion.

2 Phase transition of coupled star networks

In heterogeneous networks, such as scale-free networks, hubs play the dominate roles. The process of synchronization on scale-free networks is explosive with a hysteresis behavior as shown in Fig. 1a. The single star network which gets the essential properties of hubs had been used to investigate the intrinsic mechanism of this kind of phase transition; the route to synchronization in a star network is similar to that in the scale-free networks as shown in Fig. 1b. Based on the Watanabe–Strogatz approach (see Sect. 3), the upper limit of the forward critical coupling strength

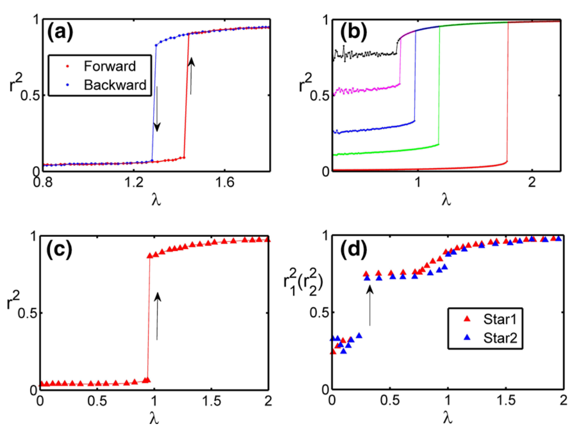

Fig. 1 (color online) **a** The forward and backward continuation diagrams for the scale-free network with $N = 10^3$, $\langle k \rangle = 6$, the exponent of degree distribution is $\gamma = 3$, and the natural frequency of each node is equal to its degree in the network. **b** The order parameter against the coupling strength with different initial states for the star network with $N = 11$, the natural frequencies of the hub and leaves are set to be 10 and 1, respectively. **c** The order parameter against the coupling strength for the coupled star network with the same size $N = 12$. **d** The order parameter of star 1 (r_1) and star 2 (r_2) against the coupling strength with $K_1 = 5$, $K_2 = 5$. The dynamical model of (**c**) and (**d**) is used by Eq. (1), where $\lambda_1 = \lambda_2 = \lambda_0$, r in (**c**) is the whole order parameter of the coupled star network and the order parameters $r_{1,2}$ in (**d**) are defined by Eq. (2)

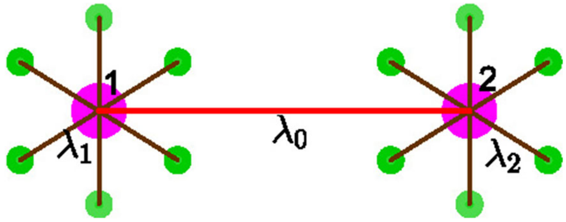

Fig. 2 A diagrammatic sketch of the coupled star network, the red solid circle corresponds to the hub, the green solid circle is the leaf, and the line is the coupling strength. λ_1 is the coupling strength in star 1, λ_2 is the coupling strength in star 2, and λ_0 represents the coupling strength between two hubs, respectively

of phase transition can be calculated analytically, i.e., $\hat{\lambda}_c^f = \frac{\Delta\omega}{\sqrt{2K+1}}$ [23]. Obviously, the forward critical coupling strength of the synchronization in the star network is influenced by its size. However, the forward critical coupling strength on the scale-free network is determined by many factors; apart from the size of the network, it can also be influenced by the basin of attractions of the bistability in the hysteresis regime and the exponent of degree distribution. These facts indicate that the single star network is not enough to investigate the intrinsic mechanism of the synchronization in the scale-free network.

Many heterogeneous networks have multiple hubs which interact and compete with each other. The influences of the hubs on the process of the synchronization in heterogeneous networks are still unknown. To address this question, we design a network which consists of several star networks with the hubs linked directly. In the following, we consider the simplest case of two coupled star networks, and the coupling structure is shown in Fig. 2. In this case, namely star 1 and star 2, the hubs of two star networks are coupled directly. The dynamical equations of the model can be written as

$$\begin{aligned}
\dot{\theta}_{h_1} &= \omega_{h_1} + \lambda_1 \sum_{j_1=1}^{K_1} \sin(\theta_{j_1} - \theta_{h_1}) + \lambda_0 \sin(\theta_{h_2} - \theta_{h_1}),\\
\dot{\theta}_{j_1} &= \omega_1 + \lambda_1 \sin(\theta_{h_1} - \theta_{j_1}), \quad 1 \le j_1 \le K_1,\\
\dot{\theta}_{h_2} &= \omega_{h_2} + \lambda_2 \sum_{j_2=1}^{K_2} \sin(\theta_{j_2} - \theta_{h_2}) + \lambda_0 \sin(\theta_{h_1} - \theta_{h_2}),\\
\dot{\theta}_{j_2} &= \omega_2 + \lambda_2 \sin(\theta_{h_2} - \theta_{j_2}), \quad 1 \le j_2 \le K_2,
\end{aligned} \tag{1}$$

where $\theta_{h_1}, \theta_{h_2}, \theta_{j_1}, \theta_{j_2}$ and $\omega_{h_1}, \omega_{h_2}, \omega_{j_1}, \omega_{j_2}$ are phases and natural frequencies of the hub and leaf nodes in star 1 and star 2, respectively. K_1, K_2 and λ_1, λ_2 are the number of leaf nodes and coupling strength for star 1 and 2. λ_0 is the coupling strength between the two stars. Throughout this paper, we set $\omega_{h1} = K_1$, $\omega_{h2} = K_2$, $\omega_{j1} = \omega_{j2} = 1$.

To describe the degree of the synchronization of a single star, we define the order parameter as

$$\begin{aligned}
Z_m(t) &\equiv r_m(t) e^{i\Phi_m(t)}\\
&= \frac{1}{K_m+1}\left(e^{i\theta_{hm}} + \sum_{j=1}^{K_m} e^{i\theta_{jm}}\right), \quad m = 1, 2.
\end{aligned} \tag{2}$$

Similarly, we define the local order parameter of the leaf nodes as

$$Z_{Lm}(t) \equiv r_{Lm}(t) e^{i\Phi_{Lm}(t)} = \frac{1}{K_m}\sum_{j=1}^{K_m} e^{i\theta_{jm}}, \quad m = 1, 2. \tag{3}$$

It is worth noting that the single star is synchronous globally only if $r_m(t) = 1$ and the leaf nodes become completely synchronous if $r_{Lm}(t) = 1$.

To depict the phase transition in this coupled star network [13], we first assume that $\lambda_1 = \lambda_2 = \lambda_0 \equiv \lambda$. The discontinuous phase transition from the neutral state to the synchronous state in a single star network is shown in Fig. 1b [23]. Here the neutral state means a central point in the two-dimensional order-parameter space that the two eigenvalues of such point are purely imaginary. Correspondingly, in the original phase-oscillator space the neutral state is a special state that all the Lyapunov exponents of the system are zero. A large class of neutral periodic orbits exist in the phase space and are determined by the initial states. Both the order parameter of the neutral state and the forward critical coupling strength for the phase transition are different from each other in various initial states.

In the coupled star network, the order parameter of the whole network will also change suddenly at a critical coupling, where all the nodes become synchronous as shown in Fig. 1c. However, the process of synchronization is not the same as that of the single star network. As shown in Fig. 1d, the synchronization for star

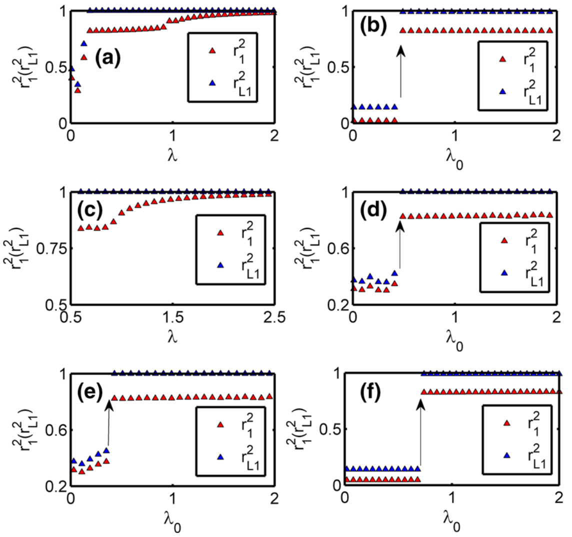

Fig. 3 (color online) The order parameter of star 1 (r_1) and the local order parameter of leaf nodes of star 1 (r_{L1}) against the coupling strength λ or λ_0 with different coupled forms when $K_1 = 10$, $K_2 = 9$, $\lambda_1 = \lambda_2 = \lambda$. **a** $\lambda_0 = \lambda$, bidirectionally coupled with the star 2. **b** $\lambda = 0.6$, bidirectionally coupled with the star 2. **c** $\lambda_0 = 1$, bidirectionally coupled with the star 2. **d** $\lambda_1 = \lambda_2 = 0.6$, unidirectionally coupled by the star 2. **e** $\lambda_1 = 0.6$, $\lambda_2 = 0.8$, unidirectionally coupled by the star 2. **f** $\lambda_1 = 0.6$, $\lambda_2 = 0$, unidirectionally coupled by the hub of star 2

1 or star 2 in the coupled star network is divided into two steps. At the first step, the state of the leaf nodes changes from the incoherent state to the in-phase state, where the phases of all the leaf nodes in each star become uniform. This in-phase state was observed as a limit cycle in the low-dimensional order-parameter space in the single star [23]. Hence, the local order parameter of leaf nodes $r_{L1} = 1$ is shown in Fig. 3a. With the increase in the coupling strength, the hub joins in the in-phase group and the system becomes synchronous gradually as the second step, which is shown by the order parameter of the star 1 $r_1 = 1$ in Fig. 3a. The second step of the transition from the in-phase state to the synchronous state also exists in a single star network with a phase-shift coupling [23]. For the latter case, when the phase shift ($0 < \alpha < 0.5\pi$) is introduced into the coupling function, all the leaf nodes become condensed (in-phase) once the coupling strength $\lambda > 0$. The phase transition process in a single star with a nonzero phase shift can be considered as a bifurcation from the in-phase state (limit cycle) to the globally synchronous state (fixed point) in the order-parameter space.

As a matter of fact, the emergence of the in-phase state is closely related to the coupling between the two star subnetworks. To confirm this argument, we first keep the coupling strength within each star $\lambda_1 = \lambda_2 \equiv \lambda$ fixed and change the coupling strength λ_0 between the hubs. As a result, the transition to the in-phase state takes place as shown in Fig. 3b. We can then keep $\lambda_0 \equiv \lambda'$ to be constant and adjust the coupling strength $\lambda_1 = \lambda_2 \equiv \lambda$ within each star; we hence observe the transition from the in-phase state to the synchronous state as shown in Fig. 3c, which corresponds to the second step of synchronization.

Furthermore, to investigate the mechanism of the first step of the phase transition, the results of numerical simulations suggest that the transition to synchronization within each star is independent, which implies that the specific value of λ_1 or λ_2 has no influence on the route to synchronization in the other star network (Fig. 3d–f). Therefore, we just pay our particular attentions to the impact caused by the coupled hubs. For simplicity, we set $\lambda_2 = 0$ within the star 2 and only discuss the dynamical transition in star 1. Under this assumption, the dynamical evolution of the reduced system reads

$$\begin{aligned}
\dot{\theta}_{h_1} &= \omega_{h_1} + \lambda \sum_{j_1=1}^{K_1} \sin(\theta_{j_1} - \theta_{h_1}) + \lambda_0 \sin(\theta_{h_2} - \theta_{h_1}),\\
\dot{\theta}_{j_1} &= \omega_1 + \lambda \sin(\theta_{h_1} - \theta_{j_1}), \quad 1 \le j_1 \le K_1,\\
\dot{\theta}_{h_2} &= \omega_{h_2}.
\end{aligned} \tag{4}$$

We emphasize that this simplified model (4) is a generalized single star network, with one special leaf node of distinct natural frequency and unidirectional coupling.

By introducing the phase differences of the system above as $\phi_i = \theta_i - \theta_{h_1}$, $\alpha = \theta_{h_2} - \theta_{h_1}$, the order parameter of star 1 in the phase difference coordinate can be redefined as $z_1 = r_1 e^{i\Phi} = \frac{1}{N}\sum_{i=1}^{N} e^{i\phi_i}$, where $N = K_1$. It is instructive to rewrite Eq. (4) in the phase difference system as

$$\dot{\phi}_j = f e^{i\phi_j} + g + \bar{f} e^{-i\phi_j}, \quad j = 1, \ldots, N, \tag{5}$$

where $f = i\frac{\lambda}{2}$, $g = \Delta\omega - \lambda_0 \sin\alpha - \frac{N\lambda}{2i}(z_1 - \bar{z}_1)$, $\Delta\omega = \omega_1 - \omega_h$. Based on the Watanabe–Strogatz theory, the evolution of the order parameter z_1 in the finite-size system Eq. (22) reads

$$\dot{z_1} = i\Delta\omega z_1 - \frac{\lambda}{2}({z_1}^2 - 1) - \frac{N\lambda}{2}(z_1 - \bar{z_1})z_1 - i\lambda_0 z_1 \sin\alpha, \tag{6}$$
$$\dot{\alpha} = \Delta\omega' - \frac{N\lambda}{2i}(z_1 - \bar{z_1}) - \lambda_0 \sin\alpha,$$

where $\Delta\omega' = \omega_{h_2} - \omega_{h_1}$. By setting $z_1 = x + iy$, it is convenient to describe the dynamics in the three-dimensional $(x,\ y,\ \alpha)$ phase space, which yields

$$\dot{x} = -\Delta\omega y - \frac{\lambda}{2}(x^2 - y^2 - 1) + N\lambda y^2 + \lambda_0 y \sin\alpha,$$
$$\dot{y} = \Delta\omega x - \lambda xy - N\lambda xy - \lambda_0 x \sin\alpha,$$
$$\dot{\alpha} = \Delta\omega' - N\lambda y - \lambda_0 \sin\alpha. \tag{7}$$

Noting that system (7) has the quasi-Hamiltonian peculiarity [15], i.e., Eq. (7) remains invariant under the time-reversal transformation R, which can be decomposed into $R = TW$ with $T : t \longmapsto -t$ and $W : (x, y, \alpha) \longmapsto (-x, y, \pm\pi - \alpha)$. Then, the trajectories of the system are also time reversible, and the volume of phase space is conserved for reversible trajectories which cross the invariant set $x = 0, \alpha = \pm\pi/2$ more than once.

3 The Watanabe–Strogatz theory and low-dimensional dynamics of order parameter

Recently, the issue of low-dimensional dynamics was reopened by Ott and Antonsen [24] with the discovery of an ansatz that collapses the infinite-dimensional Kuramoto model to a two-dimensional system of ODEs. However, whether the ODEs can be used for systems with a finite size cannot be directly implied from the Ott–Antonsen ansatz.

For the system with a finite size $N = K$, the original microscopic dynamical state can be reduced to a macroscopic collective state by the Watanabe–Strogatz approach [25,26]. At the same time, the governing equations of the system can be generated by this method. We will illustrate the Watanabe–Strogatz approach by the Möbius group action [32,33]. The class of identical oscillators are governed by the following equations of motion

$$\dot{\varphi}_j = f\mathrm{e}^{i\varphi_j} + g + \bar{f}\mathrm{e}^{-i\varphi_j}, \quad j = 1, \ldots, N, \tag{8}$$

where the analytically complex-valued 2π-periodic function f with respect to the phases $\varphi_1, \ldots, \varphi_N$ and the over bar represents complex conjugation, g is a smooth real- valued function due to $\dot{\varphi}_j$ is real. Then the phases $\varphi_j(t)$ are governed by the action of the Möbius transformation

$$\mathrm{e}^{i\varphi_j(t)} = M_t(\mathrm{e}^{i\theta_j}) \tag{9}$$

where $j = 1, \ldots, N$, and M_t denote a one-parameter family of Möbius group and θ_j is a constant value which is invariant for the system.

Parameterizing the one-parameter family of Möbius transformations can be written as

$$M_t(w) = \frac{\mathrm{e}^{i\psi}w + \eta}{1 + \bar{\eta}\mathrm{e}^{i\psi}w}, \tag{10}$$

where $|\eta(t)| < 1$ and $\psi(t) \in R$, and

$$w_j = \mathrm{e}^{i\theta_j}. \tag{11}$$

To verify that Eq. (10) gives an exact solution of Eq. (8), we obtain the time derivative of $\varphi_j(t) = -i \log M_t(w_j)$, noting that w_j is constant,

$$\dot{\varphi_j} = \frac{\dot{\psi}\mathrm{e}^{i\psi}w_j - i\dot{\eta}}{\mathrm{e}^{i\psi}w_j + \eta} + \frac{(i\dot{\bar{\eta}} - \bar{\eta}\dot{\psi})\mathrm{e}^{i\psi}w_j}{1 + \bar{\eta}\mathrm{e}^{i\psi}w_j}. \tag{12}$$

From the inverse mapping

$$w = M^{-1}(\mathrm{e}^{i\varphi}) = \mathrm{e}^{-i\psi}\frac{\mathrm{e}^{i\varphi} - \eta}{1 - \bar{\eta}\mathrm{e}^{i\varphi}}, \tag{13}$$

then we have

$$\mathrm{e}^{i\psi}w_j = \frac{\mathrm{e}^{i\varphi_j} - \eta}{1 - \bar{\eta}\mathrm{e}^{i\varphi_j}}, \tag{14}$$

which can be substituted into Eq. (12), we get

$$\dot{\varphi_j} = R\mathrm{e}^{i\varphi_j} + \frac{\dot{\psi} + i\bar{\eta}\dot{\eta} - \eta(i\dot{\bar{\eta}} - \bar{\eta}\dot{\psi})}{1 - |\eta|^2} + \bar{R}\mathrm{e}^{-i\varphi_j}, \tag{15}$$

where $R = (i\dot{\bar{\eta}} - \bar{\eta}\dot{\psi})/(1 - |\eta|^2)$.

Note that Eq. (15) falls precisely into the algebraic form required by Eq. (8). Thus, to derive the desired

ODEs for $\eta(t)$ and $\psi(t)$, we now substitute Eq. (15) into Eq. (8). Explicitly,

$$f = \frac{i\dot{\bar{\eta}} - \bar{\eta}\dot{\psi}}{1-|\eta|^2}, \qquad g = \frac{\dot{\psi} + i\bar{\eta}\dot{\eta} - \eta(i\dot{\bar{\eta}} - \bar{\eta}\dot{\psi})}{1-|\eta|^2}. \tag{16}$$

System (16) can be algebraically rearranged to give

$$\begin{aligned} \dot{\eta} &= i(f\eta^2 + g\eta + \bar{f}), \\ \dot{\psi} &= f\eta + g + \bar{f}\bar{\eta}. \end{aligned} \tag{17}$$

Through these new variables, one can write the order parameter as

$$z(t) = \frac{1}{N}\sum_{j=1}^{N} e^{i\varphi_j} = \frac{1}{N}\sum_{j=1}^{N} \frac{e^{i\psi}e^{i\theta_j} + \eta(t)}{1 + \bar{\eta}(t)e^{i\psi}e^{i\theta_j}}, \tag{18}$$

Equation (17) together with Eq. (18) can completely determine the evolution of the system for given initial conditions $\eta(0)$, $\psi(0)$ and N constants θ_j, $1 \le j \le N$. By choosing the following constants, the order parameter (18) can be further simplified,

$$\theta_j = 2\pi\frac{j-1}{N}, \quad 1 \le j \le N. \tag{19}$$

With this choice, the order parameter (18) reads

$$z(t) = \eta(t)(1 + I), \tag{20}$$

where $I = (1 - |\eta(t)|^{-2})/(1 \pm (e^{i\psi}\bar{\eta}(t))^{-N})$, "−" the case with even N and "+" corresponding to odd N. For large N, $I \ll 1$, the order parameter $z(t)$ can be approximated as

$$z(t) \approx \eta(t), \quad \text{for } N \gg 1. \tag{21}$$

From the analysis above, the evolutions of a finite-size system are equivalent to the following equation

$$\dot{z} = i(fz^2 + gz + \bar{f}). \tag{22}$$

This reduced equation is consistent with the Ott–Antonsen ansatz for systems with an infinite size [28].

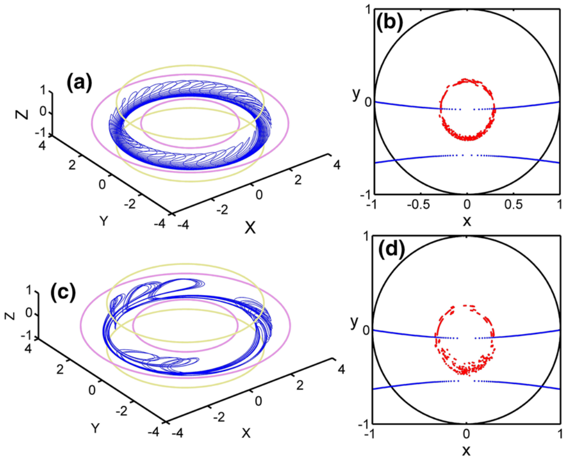

Fig. 4 (color online) **a** and **c** The phase space with $\lambda = 0.6$, $\lambda_0 = 0$ or 0.64, respectively, and $K_1 = 10$. The blue lines are the trajectories of model (4) with the transformation $X(t) = (3 + x(t)\cdot\cos(\alpha(t)))$, $Y(t) = (3 + x(t)\cdot\sin(\alpha(t)))$, $Z(t) = \alpha(t)$, other color lines are the boundary of it. **b** and **d** The Poincare section of them when $\alpha = \frac{3\pi}{2}$. The red points are the trajectories in this section; the blue lines are $\dot{x} = 0$

4 Dynamics of transition from the neutral state to the in-phase state

In Eq. (7), by setting $\dot{x} = 0$, $\dot{y} = 0$ and $\dot{\alpha} = 0$ when $\lambda_0 \neq 0$, we can obtain four fixed points. However, all the fixed points are nonphysical due to the fact that the modulus $|z| > 1$. Without steady solutions in Eq. (7), the system cannot reach the synchronous state. Additionally, when $\lambda_0 = 0$, x, y are decoupled from α and there is the periodic trajectory or quasiperiodic torus in phase space with small λ as shown in Fig. 4a, b. For $\lambda_0 > 0$, star 1 is affected by the hub of star 2, which leads the original torus to be chaotic as shown in Fig. 4c, and the torus in the Poincare section becomes inflated as shown in Fig. 4d. Furthermore, with the increase of λ_0, the system reaches the in-phase state corresponding to a limit cycle in phase space as shown in Fig. 5a. The transition from the neutral state to the in-phase state is the bifurcation from the chaotic or quasiperiodic torus to a limit cycle in phase space. The abrupt transition and hysteresis behavior are induced by the coexistence of the torus and the limit cycle with different basins of attraction.

The torus and the limit cycle belong to the conservative and dissipative solutions, respectively. From the system with time-reversal symmetry, the separation line between these two states is the nullcline that pre-

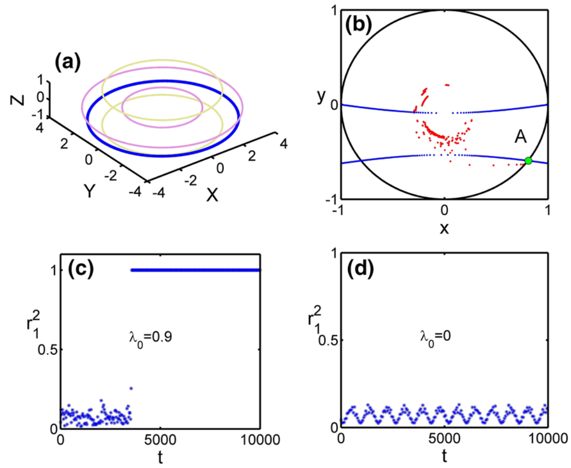

Fig. 5 (color online) **a** The phase space of model (4) with $\lambda = 0.6$, $\lambda_0 = 0.9$ and $K_1 = 10$. The blue lines are the trajectories with the transformation $X(t) = (3 + x(t) \cdot \cos(\alpha(t)))$, $Y(t) = (3 + x(t) \cdot \sin(\alpha(t)))$, $Z(t) = \alpha(t)$; other color lines are the boundary of it. **b** The Poincare section with $\alpha = \frac{3\pi}{2}$ of the phase space, the red points are the trajectories in this section, the blue lines are $\dot{x} = 0$, the fixed point A is the intersection of down blue line $\dot{x} = 0$ and the unit cycle. **c**, **d** The local order parameter of star 1 against the time with different λ_0

vents the trajectory crossing the invariant set twice, as $\dot{x} = 0$ or alternatively

$$-\Delta\omega y - \frac{\lambda}{2}(x^2 - y^2 - 1) + N\lambda y^2 + \lambda_0 y \sin\alpha = 0. \quad (23)$$

Obviously, the surface is wavy and will be the peak or bottom when $\alpha = \frac{\pi}{2}$ or $\frac{3\pi}{2}$. Hence, the largest distance between a point in the surface and a point in the torus around the center is the case with $\alpha = \frac{\pi}{2}$, and the smallest one corresponds to $\alpha = \frac{3\pi}{2}$.

Noting that in the coexistent regime of the neutral state and the synchronous state in the single star network, the orbit of the neutral state strongly depends on its initial state. The phase transition point can be estimated as the critical value where the orbits of the neutral state hit the separation surface. Based on the smallest distance between the torus and the separation surface with $\alpha = \frac{3\pi}{2}$, we have

$$x^2 = (2N + 1)y^2 - (\lambda_0 + \Delta\omega)\frac{2y}{\lambda} + 1. \quad (24)$$

Let $b = -(\lambda_0 + \Delta\omega)2/\lambda$. Due to the conservation of the phase volume of the torus, we can approximately consider that the largest order parameter in neutral states is

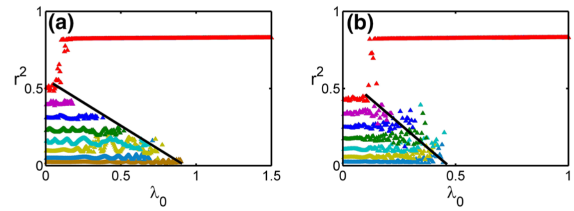

Fig. 6 (color online) The order parameter of star 1 against the coupling strength λ_0 with different initial states, **a** with $K_1 = 10$, $K_2 = 10$, $\lambda_1 = \lambda_2 = \lambda = 0.5$, unidirectionally coupled by the star 2, **b** with $K_1 = 10$, $K_2 = 8$, $\lambda_1 = \lambda_2 = \lambda = 0.8$, bidirectionally coupled with the star 2. Different color triangle shapes represent different initial values of order parameter, and they are approximately invariant before the critical point λ_{0c}; the black line represents the theoretical prediction of the linear relationship between initial values of order parameter and the critical point λ_{0c}

equal to its initial state r_0; we get the distance d between the bottom of the separation surface $r_{\min}$ and the torus with the order parameter r_0,

$$\begin{aligned} d &= r_{\min} - r_0 \\ &= \frac{2[b^2 + b\sqrt{b^2 - 4(2N+1)} - (4N+2)(4N+4)]}{(4N+2)^2} \\ &\quad + 1 - r_0. \end{aligned} \quad (25)$$

The critical transition point λ_{0c} can be determined by $d \leq 0$, where the separation surface and the torus intersect with each other. If the number of leaf nodes $N \gg 1$, $r_{\min} \approx \frac{b}{2N}$, which means that the order parameter r has a linear relation with the critical coupling strength λ_{0c} when the number of leaves is large enough.

To illustrate the process of the transition, the dynamical manifestations are shown in Figs. 4 and 5. In the case of $\lambda_0 = 0$, the hub of star 2 does not affect the behavior of star 1 as shown in Fig. 4a, b, and star 1 is in the neutral stable state with the trajectories in phase space regular and periodic. When $\lambda_0 = 0.64$, the hub of star 2 has a larger impact on that of star 1, and the trajectories in phase space become chaotic and irregular, as exhibited in terms of the Poincare section, the red points correspond to the trajectories in the section jitter and expand greatly as shown in Fig. 4d. Meanwhile, the separated surface in the section is the down blue line upwards with the increasing of λ_0 constantly, implying that the volume of the basin of attraction of the in-phase state in phase space increases and the volume of the basin of attraction of the neutral state decreases. In the critical case of the system when $\lambda_0 = \lambda_{0c}$, the trajectories in phase space will hit the separated surface and evolve to the limit cycle which corresponds to the in-phase state, and finally, the phase transition occurs as shown in Fig. 5.

Since the dynamical process of the transition to synchronization of model (4) has been illustrated clearly, three points should be emphasized. First, no stable fixed points exist in phase space, and the green point A in the Poincare section is the limit cycle solution which is related to the in-phase state. Second, the torus of the neutral state in phase space becomes chaotic and inflated. Third, with the increasing of the coupling strength between the hubs, the basin of attraction of the in-phase state will enlarge, and the basin of attraction of the neutral state will shrink. According to three factors above, the mechanism of the transition from the neutral state to the in-phase state is clearly revealed, which can be further checked by the linear relation between the critical coupling λ_{0c} and the initial condition r_0 as shown in Fig. 6. The linear relation exists both in the cases of the unidirectionally and the bidirectionally coupled star networks. It is verified that the linear relation obtained by numerical computations is consistent with the previous results, which proves that the mechanism of model (4) is reasonable.

5 Conclusion

To summarize, we investigate the dynamics of phase transition in the star network with the hubs interacting each other. The coupling between the system can accelerate the progress of the synchronization in each single star network. Furthermore, the low-dimensional dynamical equation of the system was derived in terms of Watanabe–Strogatz theory, and the microscopic mechanism of phase transition can be clearly clarified. Theoretical analysis shows that the phase transition of the system undergoes two different steps, the former is from the incoherent state to the in-phase state corresponding to the bifurcation from the chaotic or quasiperiodic torus to a limit cycle in the order-parameter phase space, whereas the latter is from the in-phase state to the synchronous state equivalent to the bifurcation from the limit cycle to the fixed point in phase space. This bifurcation can be reflected by the relationship between the critical point λ_{0c} and the initial condition r_0. These results are helpful for understanding the phase transition in more general heterogeneous networks.

Acknowledgements This work was partially supported by the NSFC Grants No. 11475022, and the Scientific Research Funds of Huaqiao University (Grant Nos. 15BS401 and 600005-Z17Y0064).

References

1. Kuramoto, Y.: Chemical Oscillations, Waves and Turbulence. Springer, Berlin (1984)
2. Acebron, J.A., Bonilla, L.L., Vicente, C.J.P., Ritort, F., Spigler, R.: The Kuramoto model: a simple paradigm for synchronization phenomena. Rev. Mod. Phys. **77**, 137 (2005)
3. Strogatz, S.H.: From Kuramoto to Crawford: exploring the onset of synchronization in populations of coupled oscillators. Physica D **143**, 1 (2000)
4. Pikovsky, A., Rosenblum, M., Kurths, J.: Synchronization: A Universal Concept in Nonlinear Sciences. Cambridge University Press, Cambridge (2001)
5. Dorogovtsev, S.N., Goltsev, A.V., Mendes, J.F.F.: Critical phenomena in complex networks. Rev. Mod. Phys. **80**, 1275 (2008)
6. Arenas, A., Diaz-Guilera, A., Kurths, J., Moreno, Y., Zhou, C.: Synchronization in complex networks. Phys. Rep. **469**, 93 (2008)
7. Zheng, Z., Hu, G., Hu, B.: Phase slips and phase synchronization of coupled oscillators. Phys. Rev. Lett. **81**, 5318 (1998)
8. Dai, Q., Liu, Q., Cheng, H., et al.: Chimera states in a bipartite network of phase oscillators. Nonlinear Dyn. **92**(2), 741–749 (2018)
9. Rodrigues, F.A., Peron, T.K.D.M., Ji, P., et al.: The Kuramoto model in complex networks. Phys. Rep. **610**, 1–98 (2016)
10. Boccaletti, S., Almendral, J.A., Guan, S., et al.: Explosive transitions in complex networks' structure and dynamics: percolation and synchronization. Phys. Rep. **660**, 1–94 (2016)
11. Silber, M., Fabiny, L., Wiesenfeld, K.: Stability results for in-phase and splay-phase states of solid-state laser arrays. J. Opt. Soc. Am. B **10**, 1121 (1993)
12. Strogatz, S.H., Mirollo, R.E.: Splay states in globally coupled Josephson arrays: analytical prediction of Floquet multipliers. Phys. Rev. E **47**, 220 (1993)
13. Gómez-Gardeñes, J., Gómez, S., Arenas, A., Moreno, Y.: Explosive synchronization transitions in scale-free networks. Phys. Rev. Lett. **106**, 128701 (2011)
14. Omel'chenko, O.E., Wolfrum, M.: Nonuniversal transitions to synchrony in the Sakaguchi–Kuramoto model. Phys. Rev. Lett. **109**, 164101 (2012)
15. Topaj, D., Pikovsky, A.: Reversibility vs. synchronization in oscillator lattices. Physica D **170**, 118 (2002)
16. Zhang, X., Hu, X., Kurths, J., Liu, Z.: Explosive synchronization in a general complex network. Phys. Rev. E **88**, 010802(R) (2013)

17. Hu, X., et al.: Exact solution for first-order synchronization transition in a generalized Kuramoto model. Sci. Rep. **4**, 7262 (2014)
18. Leyva, I., et al.: Explosive first-order transition to synchrony in networked chaotic oscillators. Phys. Rev. Lett. **108**, 168702 (2012)
19. Li, P., Zhang, K., Xu, X., Zhang, J., Small, M.: Reexamination of explosive synchronization in scale-free networks: the effect of disassortativity. Phys. Rev. E **87**, 042803 (2013)
20. Peron, T.K.D.M., Rodrigues, F.A.: Explosive synchronization enhanced by time-delayed coupling. Phys. Rev. E **86**, 016102 (2012)
21. Ji, P., Peron, T.K.D.M., Menck, P.J., Rodrigues, F.A., Kurths, J.: Cluster explosive synchronization in complex networks. Phys. Rev. Lett. **110**, 218701 (2013)
22. Leyva, I., et al.: Explosive transitions to synchronization in networks of phase oscillators. Sci. Rep. **3**, 1281 (2013)
23. Xu, C., Gao, J., Sun, Y., Huang, X., Zheng, Z.: Explosive or continuous: incoherent state determines the route to synchronization. Sci. Rep. **5**, 12039 (2015)
24. Ott, E., Antonsen, T.M.: Low dimensional behavior of large systems of globally coupled oscillators. Chaos **18**, 037113 (2008)
25. Watanabe, S., Strogatz, S.H.: Integrability of a globally coupled oscillator array. Phys. Rev. Lett. **70**, 2391 (1993)
26. Watanabe, S., Strogatz, S.H.: Constants of motion for superconducting Josephson arrays. Physica D **74**, 197 (1994)
27. Bergner, A., et al.: Remote synchronization in star networks. Phys. Rev. E **85**, 026208 (2012)
28. Chen, H., Sun, Y., Gao, J., Zheng, Z., Xu, C.: Order parameter analysis of synchronization transitions on star networks. Front. Phys. **12**, 120504 (2017)
29. Burylko, O., Kazanovich, Y., Borisyuk, R.: Bifurcations in phase oscillator networks with a central element. Physica D **241**, 1072 (2012)
30. Theesar, S.J.S., Ariffin, M.R.K., Banerjee, S.: Synchronization and a secure communication scheme using optical star network. Opt. Laser Technol. **54**, 15 (2013)
31. Vlasov, V., Pikovsky, A., Macau, E.E.N.: Star-type oscillatory networks with generic Kuramoto-type coupling: a model for Japanese drums synchrony. Chaos **25**, 123120 (2015)
32. Goebel, C.J.: Comment on “Constants of motion for superconductor arrays”. Physical D **80**, 18 (1995)
33. Marvel, S.A., Mirollo, R.E., Strogatz, S.H.: Identical phase oscillators with global sinusoidal coupling evolve by Möbius group action. Chaos **19**, 043104 (2009)